# New Concept of Spray Saturation Tower for micro Humid Air Turbine Applications

W. De Paepe[a,*], F. Contino[a], F. Delattin[a], S. Bram[b,a], J. De Ruyck[a]

[a] *Vrije Universiteit Brussel, Dept. of Mechanical Engineering (MECH), Pleinlaan 2, 1050 Brussel, Belgium*

[b] *Vrije Universiteit Brussel, Dept. of Industrial Engineering Sciences (INDI), Nijverheidskaai 170, 1070 Brussel, Belgium*

**Abstract**

The micro Humid Air Turbine (mHAT) has proven to have the highest potential of all mixed air/water micro Gas Turbines (mGTs). Turning a mGT into a mHAT however requires the installation of a saturation tower. Most common saturation towers use packing material to increase the contact area between compressed air and water. The packing material however causes a pressure drop, which has a severe negative effect on the mGT performance. To limit this pressure drop, we have developed a spray tower without packing that uses nozzles to inject water in the compressed air. In this paper, we propose a design for the spray tower based on two-phase flow simulations. The two major constraints during the design were minimal pressure loss and tower size. A sensitivity analysis was performed in order to indicate the key parameters to obtain fully saturated air from the tower. Results of simulations showed that using a spray tower reduces the pressure losses when compared to a classic saturation tower. Sensitivity analysis showed that droplet diameter and injected water mass flow rate have the largest effect on the final size of the spray tower. Finally, a cross-current spray tower design was proposed for a Turbec T100 mGT because the sensitivity analysis showed that cross-current droplets injection meets the design constraints best.

*Corresponding author

*Email addresses:* wdepaepe@vub.ac.be (W. De Paepe), fcontino@vub.ac.be (F. Contino), fdelatti@vub.ac.be (F. Delattin), svend.bram@ehb.be (S. Bram), jdruyck@vub.ac.be (J. De Ruyck)

*Keywords:* micro Gas Turbine, micro Humid Air Turbine, saturation tower, spray tower, two-phase flow

## 1. Introduction

Gas Turbines (GTs) with mixed air/water as working fluid promise high electrical efficiency, high specific power output and low $NO_x$ exhaust [1]. Among these mixed air/water GTs, the Humid Air Turbine (HAT), as initially proposed by Rao [2], has proven to have the highest potential [1]. Introducing an innovative component, the saturator, in the cycle layout will enhance the GT performance. However, only one pilot plant, the Evaporative Gas Turbine (EvGT) project, has been constructed and successfully tested in Lund since the development of the HAT cycle layout. The evaporative cycle without aftercooling achieved a thermal efficiency of approximately 35% [1, 3]. Later, different variants of the HAT were developed: the Cascaded Humidified Advanced Turbine (CHAT) [4] and the Advanced Humid Air Turbine (AHAT) [5, 6]. The CHAT cycle was developed to overcome the problem of the flow mismatch that exists between compressor and turbine in the original HAT design [4]. The AHAT cycle substitutes the intercooling from the HAT cycle by Water Atomizing inlet air Cooling (WAC) [6]. Hitachi built and tested a 4 MW-class AHAT pilot plant in Japan [7, 8]. Results of tests indicated a thermal efficiency of 40% of the power plant [7].
The effects of turning a micro Gas Turbine (mGT) into a micro Humid Air Turbine (mHAT) on the thermodynamic performance have been investigated by means of simulations [9, 10, 11, 12]. Zhang and Xiao studied the effect of the humid air on the performance of the different mGT components [9]. Parente et al. determined the beneficial effect of adding water to the cycle on the global performance and studied the thermoeconomic efficiency of the mHAT, applied on current and future technologies [10, 11]. The authors of this paper showed that the maximal potential for water injection in a mGT based HAT is 6 %wt of the compressor inlet air, which corresponds to a relative increase of thermal efficiency of 23% [12].

The saturator has been the subject of many studies performed by different researchers [13, 14, 15, 16, 17, 18, 19, 20]. Lindquist et al. developed a physical model of the saturation tower and validated this model experimentally on the saturator constructed for the EvGT project in Lund [13]. Ågren and Westermark investigated the possibility of a part-flow EvGT [14].

Parente et al. developed a code to simulate the evaporation in the saturator, using the hypothesis of a semi-ideal gas mixture [15]. Simulation results were validated against experimental results of the EvGT in Lund. Pedemonte et al. and Traverso investigated both experimentally the saturator performance on a specially designed test rig [16, 18]. Afterwards Pedemonte et al. used their results to develop empirical correlations to predict the humidification process in a pressurized saturator with packing [17]. Finally, Araki et al. designed, simulated and validated experimentally the saturator of the 4 MW-class AHAT power plant built in Japan [19, 20].

All of the previously discussed saturators or saturation towers use packing material to increase the contact area between the compressed air and the water, which will speed up the humidification process. Packing material however induces a pressure drop (approximate 400 Pa/m of packing [10]). Pressure losses in mGT have a large negative effect on mGT performance [21, 22]. For this reason, a new type of saturation tower has been developed using two-phase flow theory. Instead of increasing the contact area by using packing material, nozzles were used. The idea is that dividing the water in a large amount of small droplets will result in a large contact area between the liquid and the compressed air, which will provide the necessary surface for heat and mass transfer.

The final goal of this paper is to design the saturator for the mHAT version of the Turbec T100 mGT, installed in the labs of the Vrije Universiteit Brussel. During the design process, the main parameters of interest are saturator size and pressure drop. It is of great importance that both are lower than in a classical saturator with packing material. The secondary goal was to study the sensitivity of the humidification process to possible variations of the saturator inlet conditions. Eventually, a saturator will be constructed based upon the obtained recommendations.

In the first part of this paper, the modelling of the internal two-phase flow of the spray saturator is discussed. For every injection direction of the droplets, the considered assumptions are discussed. In the second part of this paper, the results of the different two-phase flow simulations for the different injection strategies are presented and discussed. Sensitivity analysis is performed to indicate the crucial parameters. In the final part of the paper, a conservative design for the saturator is proposed based on results of the sensitivity analysis.

## 2. Modelling

In this section, first the mHAT cycle layout is discussed in order to situate the saturator in the cycle. Secondly, the used two-phase flow model is presented. The model is based on a model developed by one of the authors [23]. Rather than fully calculating the behaviour of the droplets by means of 3D-computational fluid dynamics, a simplified 1D-model is used to predict the optimal size of the saturator for full humidification of the hot compressed air.

### *2.1. mHAT cycle layout*

The model of the mHAT cycle is based on the Turbec T100 mGT (Figure 1). Air is compressed in the compressor (1). Rather than routing the compressed air directly to the recuperator, the air is humidified in the saturator, by means of an excess of water (2). The saturated air-water mixture is preheated by the exhaust gasses in the recuperator (3). Afterwards, the air-vapour mixture is heated till maximal Turbine Inlet Temperature (TIT) by burning natural gas in the combustor (4). Expansion over the turbine (5) provides the necessary power to drive the compressor and the high speed generator for electric power production (not included in Figure 1). After preheating the compressed saturated air, exhaust gasses are used to reheat the water returning from the saturator (6). Feed water to replace the evaporated water is added to the water cycle (7).

We previously simulated the mHAT cycle, using a black box method [12]. The working parameters of the saturator can be found in Table 1. The amount of evaporated water is rather low compared to the amount of injected water (2%). The large amount of water is however necessary to provide the contact area for evaporation. This large amount of circulating water has an influence on the mHAT global performance. As indicated previously by the authors of this paper, the loss in efficiency, resulting from the auxiliary pump power for water injection, depends on the total amount of circulating water, but also on the used injection pressure [12]. For a total injected amount of water of 2.5 kg/s at 0.5 bar pressure difference, losses are equal to 0.1% absolute efficiency decrease, which is low compared to the 7% absolute efficiency increase due to the water injection [12].

### *2.2. Two-phase flow model*

To model the saturator, a previously developed method by one of the authors, the 1D Non-Adiabatic Annular Two-Phase Model has been modified

[23]. The model was constructed in the scope of the REgenerative EVAPoration (REVAP®) project [24]. The goal of this project was the development of a humidified GT without saturator.

Bram presented in his thesis a review on annular two-phase flow models [23]. In addition, other work exists in literature on the modelling of cooling towers:

- Fossa and Niksiar and Rahimi both modelled co-current gas spray cooling [25, 26];
- Fisenko et al. modelled a mechanical draft counter-current cooling tower [27];
- Fisenko and Brin made a model for a cross-flow cooling tower [28].

Nevertheless, none of these models found in literature is considered complete enough to simulate the humidification process in the considered spray tower. Therefore, the authors decided to develop their own model. The used correlations for specific phenomena, like droplet deposition, film entrainment and heat and mass transfers, were however taken from literature [23].

The model distinguishes three different components in the flow:

- Gas core
- Liquid film
- Dispersed droplets

Each different component is seen in the model as a separated phase, which has a specific mass, momentum and energy. Different types of interaction exist between the different components of the flow (Figure 2). In this case, the saturator is considered adiabatic and perfectly insulated from the environment, so the heat exchange with the surrounding can be neglected.

In the case where nozzles are used to generate the droplets, there will be no uniform droplet diameter. Each different type of nozzle produces a specific distribution of droplets. A possible way to describe this, is using a discrete distribution of droplets with several representative diameters. All categories of droplet are thus seen as separated fractions, with own conservation equations. This would however make the model too complex. The final goal is to give a conservative design of the saturator and not to describe the

exact internal behaviour of the droplets. Another possible solution is using the Sauter mean diameter ($d_s$) of the droplets. This diameter has the same ratio of surface to mass as the total droplet population. Mathematically:

$$d_s = \frac{\sum_{j=1}^{k} n_j d_j^3}{\sum_{j=1}^{k} n_j d_j^2}, \tag{1}$$

where $n$ is equal to the amount of droplets with diameter $d_j$ and $k$ is equal to the total number of droplets categories.

The next subsections present the models made to describe the three possible injection strategies: co-, counter- and cross-current. In the co-current injection, the droplets are injected in the direction of the moving gas flow. In counter-current injection, the droplets are injected in the opposite direction of the moving gas core. In the cross-flow, the droplets are injected perpendicular to the moving gas flow.

*2.2.1. Co-current model*

Mass conservation applies over each different cross section for each component, so one can write:

$$\frac{\mathrm{d}\dot{m}_i}{\mathrm{d}x} = \dot{m}_{\mathrm{s},i} - \dot{m}_{\mathrm{l},i}, \tag{2}$$

where $i$ indicates the different component (gas, film or droplets). The source term $\dot{m}_{\mathrm{s},i}$ combines all possible sources to the specific phase. For the droplets, for example, this combines the amount of water condensation from the gas core back to the droplets together with the amount of entrained droplets in the considered section of the saturator. The loss term $\dot{m}_{\mathrm{l},i}$ combines all possible mass losses of the considered phase in the considered section. For the droplets, $\dot{m}_{\mathrm{l},i}$ is equal to the sum of the amount of water that evaporates from the droplets into the gas core and the amount of droplets that are deposited in the film.

Conservation of momentum gives

$$\frac{\mathrm{d}\left(\dot{m}_i C_i\right)}{\mathrm{d}x} + A_i \frac{\mathrm{d}p}{\mathrm{d}x} = F_i' + \dot{m}_{\mathrm{s},i} C_i - \dot{m}_{\mathrm{l},i} C_i, \tag{3}$$

where $F_i'$ is the combined force, like friction between the different components, applied on the different components. $A_i$ is the part of the cross section

occupied by different flow components. Since only one dimension is considered, the effect of gravity is only taken into account when a vertical flow is considered. Results indicated that the fraction of gravity in the momentum change is generally smaller than 12% during the evaporation process.

Finally, the energy equations are

$$\frac{\mathrm{d}\left(\dot{m}_i h_i\right)}{\mathrm{d}x} = \dot{m}_{\mathrm{s},i} h_i - \dot{m}_{\mathrm{l},i} h_i + \dot{Q}'_i + F'_i C_i, \tag{4}$$

where $\dot{Q}'_i$ is the heat exchange between the different phases.

Equations (2), (3) and (4) result into a set of 9 Ordinary Differential Equations (ODEs) with 10 unknown parameters ($\dot{m}_i$, $C_i$, $h_i$ and $p$). By differentiating the following equations, the system of ODEs can be closed [23]:

- the ideal gas law;
- the relations between mass flow rate and velocity;
- the sum of all flow sections must be equal to the saturator cross section;
- the change in molecular weight of the gas core;
- the enthalpy-temperature relation of the gas core;
- the evolution of the droplet mass.

In the case of co-current injection of the droplets, the ODEs can be solved directly, using a variable step size ODE-solver, ode15s, implemented in Matlab [29]. The stability in this application of the solver was tested in the past by Bram [23].

In the simulations, all different injection positions (Figure 3) were investigated. This means that depending on the direction of movement of the gas and droplets, gravity is excluded (Figure 3(b)) from Equations (3) and (4) or included (Figure 3, (a) and (c)).

*2.2.2. Counter-current model*

The equations described in the previous subsection (Equation 2 to 4) were also used for counter-current simulations. However in the counter-current model, the interaction with the film is neglected. The fraction of heat and

mass exchange between film and gas core is very small compared to the exchange between droplets and gas. For typical values of the inlet parameters, the mass transfer from the droplets to the gas is four order of magnitude bigger than the mass transfer from the film to the gas. Even though exchange with the film is neglected, the film flow is still considered as a loss of water to preserve mass conservation.

Unlike in the co-current case, in the counter-current case, the inlet conditions of the water are defined on the opposite side of the saturator than the air inlet conditions. This has some implication for solving the problem. Here the ODEs need to be solved in an iterative way. The major difficulty in this case is the tower length. In the co-current case, the set of ODEs can be solved over a long tower. Results of relative humidity will indicate the point of full humidification of the compressed air. This point indicates the minimal necessary saturator length. Making the saturator longer will have no effect on the outlet conditions of the stream, since thermodynamic equilibrium is achieved. In the counter-current case, a different length will result in a different final solution, meaning different outlet conditions. An additional problem is that not every combination of parameters will lead to a solution. The initial velocity of the droplets needs to be higher than in the co-current case, since the droplets have to travel against the air flow and are exposed to higher friction forces. Especially the small droplets will encounter difficulties in reaching the bottom of the saturator and will most likely turn, which changes the counter-flow into a co-current flow. Higher injection velocity requires however higher pressure difference over the nozzle.

The different considered injection schemes for simulations are summarized in Figure 4.

*2.2.3. Cross-current model*

For simulating the cross-current model, at least 2D-simulations are required, since the droplets will move in a direction perpendicular to the gas flow. However, by applying some conservative simplifications to the model, a 1D-model can be used to simulate cross-current:

- the heat and mass transfer with the film is neglected and the film flow is considered as a loss of water mass flow;
- the droplet temperature, as a conservative choice, is taken equal to the temperature of the outgoing water (78°C). Calculating the temperature profile of the droplets is not possible since 1D-simulations are

preformed, so the temperature is kept constant along the droplet trajectory. Thermodynamic simulations of the saturator have shown that the water temperature does not change much (4°C: see Table 1);

- droplets are homogeneous distributed over the length and width of the saturator. The total amount of droplets per cross section depends on the height and the initial velocity. Based upon these parameters, the residence time can be calculated. Thus in the cross flow case, the tower length also needs to be predefined, as in the counter current model;

- droplet diameters are also considered constant along the droplet trajectory. Only 2% of the total water flow rate will evaporate (Table 1) along the full length of the tower. The droplet diameter is mostly reduced within the first 15% of the saturator tower length, where most of the mass transfer occurs (Figure 11(a)). This reduction in droplet diameter is still rather limited;

- droplets are considered to have zero velocity in the compressed air flow direction. Correct relative velocity (vector sum of droplet and gas velocity) is however used to calculate the heat and mass transfer coefficients.

The assumption of zero velocity of the droplets in the compressed air flow direction is justified by simulating the droplets trajectories. The possible cross-current injection schemes are indicated in Figure 5. Figure 6 shows the different droplet trajectories in the saturator, using the different injection schemes from Figure 5. Simulations are conducted using the same inlet conditions as used in cross-current saturator simulations (see 3.1.3) and neglecting the heat and mass transfer. The x-axis is defined as the gas flow direction, while the y-axis is the injection direction. In case (b), where the gas is moving downward and droplets are injected horizontally, droplets do not reach the other side of the saturator, but are dragged along the tower, which results thus in a co-current flow. In this case, the hypothesis of zero velocity in the compressed air flow direction is no longer valid. Case (b) was not considered during simulation. In case (d), droplets are just falling back down. This results in coalescence between the up-going and the falling droplets, resulting in larger droplets and thus less contact area. In addition, there is no contact between the droplets and the compressed air in the upper section of the saturator. This will result in not fully saturated air. This case

is thus also not considered in the simulations. Finally, for cases (a) and (c), droplets will move along the cross section in the direction of the gas flow. The displacement of droplets (which is the movement of the droplets in the flow direction of the compressed air) is however limited (0.06m in case (a) and 0.14m in case (c)) compared to the total length of the tower (0.50m). The limited movement justifies the assumption of zero droplet velocity in the compressed air flow direction. In addition, there will be also no droplet coalescence. All droplets follow the same trajectory, since the gas velocity does not change much as shown in Figure 11(c), resulting in constant friction forces on the droplets along the saturator.

## 3. Results

In the first section, the results of the simulations of the saturator using the different injection principles (co-, counter- and cross-current) are presented. In this section, the focus is on the evaporation process. Only the main thermodynamic parameters are discussed. In the second section, results of the sensitivity analysis are shown. The effects of the variation of different parameters on the humidification process and pressure drop are discussed.

### *3.1. Two-phase flow simulations*

#### *3.1.1. Co-current*

Co-current spray saturator is simulated using inlet conditions from Table 1 (Figure 7). Further inlet conditions, using common nozzles and saturator size, are:

- $d_{\text{droplet}} = 0.1$ mm;
- $D_{\text{saturator}} = 0.5$ m;
- $C_{\text{droplet}} = 20$ m/s.

In the co-current case, a cylindrical saturator is assumed, since the circular cross section matches best the nozzle spray cone. In this case, to exclude the effect of gravity on the performance, a horizontal saturator, with horizontal gas and droplet flow is assumed (case (b), Figure 3).

Most of the heat and mass transfer happens just after the injection point (Figure 7(a)). At this point, the driving force – low relative humidity (Figure 7(e)), thus low vapour pressure in the gas – is very high. The higher

the relative humidity becomes, the more the mass transfer process is slowed down. Due to this high evaporation rate, droplet, film and gas temperature all decrease, because all energy is necessary to evaporate the water (Figure 7(b)). Final equilibrium temperature for droplets, film and gas is below their initial temperature.

The droplets continuously slow down, due to the friction with the gas (Figure 7(c)). In the first 5 cm of the saturator, the gas will speed up due to the friction with the droplets and the evaporation (increasing gas volume). After this 5 cm, the friction with the wall and film starts to become more important, resulting in a decreasing gas velocity. Film velocity remains almost constant and very low.

Droplet diameter only varies little during the evaporation process (Figure 7(d)). The small droplet diameter variation (max. 0.6%) is a result of the large amount of injected water. Only 2% or 0.045 kg of the total amount of injected water will evaporate. After 0.20 m, the compressed air reaches full saturation (100% relative humidity, see Figure 7(e)). Once this point is reached, the gas mass flow remains constant, but the droplet mass flow rate is continuously decreasing, due to the deposition of droplets in the film.

Pressure increases during the evaporation process, as indicated on Figure 7(f). The behaviour of the pressure is rather complex and needs some additional study. For this reason, the saturator has been elongated (5m total length) to better show the effect of water injection on the pressure.

The pressure is a complex parameter, whose behaviour is influenced by several effects that counteract. On the one hand, pressure will increase due to the evaporation of the water. On the other hand, pressure will decrease due to the friction between the gas core and the wall (or film) and the lower temperature. Finally, there is also the effect of the presence of the droplets. Pressure simulations show the effect of the droplets injection and the evaporation process on velocity and pressure (Figure 8 and 9). In case $C_{\text{droplet,init}} > C_{\text{gas,init}}$, pressure will first increase (Figure 8(a) and (b)). Finally, after the pressure has reached a maximum, it starts to decrease. In this phase, droplets, film and gas are in thermal equilibrium (same temperature and relative humidity of 100%, so that there is no more heat and mass transfer). There is no more friction between the droplets and the gas core since $C_{\text{droplet}} = C_{\text{gas}}$ (Figure 8(a)). The only remaining effect is the friction between the gas core and the film/wall, which will decrease the pressure(Figure 8(b)). Since the velocity difference between gas core and film is low, pressure losses are limited in this region (0.06 Pa/m). In the case where $C_{\text{droplet,init}} < C_{\text{gas,init}}$, pressure de-

creases first largely (Figure 9(a) and (b)), until the equilibrium is reached. In the second phase, as mentioned before, pressure losses are limited, explaining the change in pressure loss gradient (Figure 9(b)).

*3.1.2. Counter-Current*

Like in the co-current case, the inlet conditions of Table 1 are used to simulate the counter-current saturator (Figure 10). Further inlet conditions are:

- $d_{\text{droplet}} = 0.5$ mm;
- $D_{\text{saturator}} = 0.5$ m;
- $L_{\text{saturator}} = 0.5$ m;
- $C_{\text{droplet}} = 8$ m/s.

Finally, injection scheme (a) from Figure 4 is used to generate the results of Figure 10.

Most of the mass and heat transfer occurs at the compressed air inlet (Figure 10(a)), due to the large driving force (low relative humidity and big temperature difference, Figure 10(b) and (d)). The temperature of the outgoing saturated compressed air is 82°C. Both gas and droplet velocity decrease continuous due to friction (Figure 10(c)). Droplet diameter reduces 0.8% along the saturator axis Figure 10(d). This is more than in the co-current case (0.6%), but since the outgoing air temperature is higher, more water is evaporated to reach full saturation after 0.5m (Figure 10(e)). Pressure loss is larger than in the co-current case, since the gas and droplets are moving in the opposite direction, resulting in larger friction forces (119 Pa, Figure 10(f)).

*3.1.3. Cross-current*

The inlet conditions as described in Table 1 are used for cross current flow simulations, except for the droplet temperature (Figure 11). As mentioned before, the droplet temperature is kept constant and equal to the outlet temperature ($T_{\text{d}}$=78°C). For the simulations, shown in Figure 11, injection scheme (c) from Figure 5 is used. Further inlet conditions are:

- $d_{\text{droplet}} = 0.5$ mm,
- $H_{\text{saturator}} = 0.5$ m,

- $W_{\text{saturator}} = 0.3$ m,
- $L_{\text{saturator}} = 0.5$ m,
- $C_{\text{droplet}}$=20 m/s.

In the cross-current flow, a rectangular cross section has been used, for the ease of simulations. The final cross section design will depend on the spray cone of the nozzle. The cross section should match the spray cone, in order to obtain an optimal contact between the air flow and injected droplets.

Since the droplet temperature is kept constant and droplets move in a direction perpendicular to the gas flow, droplet temperature, mass flow and velocity are not shown on Figure 11.

The mass transfer occurs again in the first 10 cm of the saturator (Figure 11(a)), due to the large driving force (low relative humidity, Figure 11(d)). The compressed air cools down, till the equilibrium temperature of 78°C is reached (Figure 11(b)). According to Figure 11(d), saturation is already reached after 0.13m. Shortening the tower is however not possible. If the tower length is changed, the amount of injected water also needs to be changed, since we assume a homogeneous distribution of the droplets. Changing this amount however, will affect the performance of the water heater of the mHAT, and will results in a lower mHAT performance.

The gas is slowed down by the friction between the gas core and wall and droplets, since the droplets are moving perpendicular to the gas flow (Figure 11(c)). Pressure simulations indicate that the pressure decreases over the length of the saturation tower due to the friction with the wall and the droplet (Figure 11(e)). Total pressure losses are however very low (less than 40 Pa or 0.01% of the total pressure).

### *3.2. Sensitivity analysis*

For the sensitivity analysis, all different input variables have been varied over a specific range. The parameters are droplet diameter ($d_{\text{droplet}}$) and velocity ($C_{\text{droplet}}$), saturator cross section ($A_{saturator}$), water and air mass flow rate ($\dot{m}_{\text{water}}$ and $\dot{m}_{\text{air}}$), water and air temperature ($T_{\text{water}}$ and $T_{\text{air}}$) and pressure ($pressure$). The range was chosen based on the possible physical variations of the parameters.

One can divide the parameters into two main groups: the design parameters and the thermodynamic parameters. The design parameters, $d_{\text{droplet}}$, $A_{saturator}$, $\dot{m}_{\text{water}}$, $T_{\text{air}}$ and $C_{\text{droplet}}$, can be chosen in order to minimize the size

of the saturator and to minimize the pressure drop. In the sensitivity analysis, these parameters are varied in order to gain insight in the effect of these parameters on the saturator length. The thermodynamic properties of the compressed air on the other hand are controlled by the mGT control system. The control of these parameters is thus not within reach of the designer of the saturator; however variation of these parameters is likely. Depending on the inlet air conditions and the operator chosen set points (produced electrical power), the mGT control system will change the rotation speed of the compressor, which will of course have an effect on compressor outlet condition and thus on the saturator inlet conditions ($T_{\text{air}}$, $pressure$ and $\dot{m}_{\text{air}}$) as well. In case there is a small variation on these parameters, compressed air leaving the saturation tower still needs to be saturated. In the sensitivity analysis, these parameters are thus varied over their operational range, to verify if the compressed air is fully humidified when leaving the saturator.

The main goal of the sensitivity analysis was to determine the effect of each parameter on the minimal length of the saturator and on the total pressure change. Saturation length is defined as the necessary tower length to achieve the full humidification. Results of parameter variation on relative humidity and pressure change for the different injection strategies – co-, counter- and cross-current injection – are presented in following subsections.

*3.2.1. Co-current*

The saturation length for co-current droplet injection is most sensitive to variations in the droplet diameter and water mass flow rate (Figure 12), while droplet velocity, saturator diameter and water mass flow rate variations have a major effect on pressure drop (Figure 13). For this sensitivity analysis of the co-current model, the inlet conditions of Table 1 are used in combination with the geometric conditions given in 3.1.1. Every time, the indicated parameter is varied over the specified range while all other parameters were kept constant to really focus on the influence of the considered parameter. In addition, interaction with the film flow has been neglected to save calculation time.

Droplet diameter ($d_{\text{droplet}}$) has a huge impact on saturation length (Figure 12) and on pressure changes (Figure 13). The droplet diameter determines the contact area for heat exchange and mass transfer. A droplet diameter twice as large results in a reduction of contact area by 4. This has a severe negative effect on heat and mass transfer, since these two phenomenons take place at the contact surface of both phases. Since smaller

droplets result in more contact surface, there will be more friction, which explains the increasing pressure changes for smaller droplet diameters.

Both droplet velocity ($C_{\text{droplet}}$) and cross section size (here in the form of the saturator diameter, $D_{\text{saturator}}$) have a rather small influence on the saturation length (Figure 12), but a large effect on pressure variations (Figure 13). The cross section determines the gas velocity. Heat and mass transfer are positively influenced by a larger velocity difference. On the other hand, this effect is not strong enough to compensate the faster moving gas core, which results in a lager saturation length. Since the saturator diameter affects the gas velocity, it has the largest effect on pressure change. A higher gas velocity results in a higher pressure increase due to the interaction with the droplets. The bigger the difference between droplet and gas velocity, the more the pressure will increase, due to higher friction forces between both. Pressure will increase since $C_{\text{droplets}} > C_{\text{gas}}$ (see section 3.1.1).

The water mass flow rate ($\dot{m}_{\text{water}}$) has a positive effect on the saturation length (Figure 12) and on pressure variations (Figure 13). More water will result in more droplets and thus more contact area, which will enhance the heat and mass transfer. The larger the injected amount of water is, the more droplets there are. All these droplets are slowed down by the gas, which will increase the pressure.

The influence of the air ($T_{\text{air}}$) and water temperature ($T_{\text{water}}$) on the saturator length and pressure variations is low (Figure 12 and Figure 13). A higher temperature has a positive effect on the heat and mass transfer, which should speed up the evaporation process. However it requires more water evaporation to achieve full humidification. So even though the evaporation process is enhanced, saturation length remains more or less constant since more water needs to evaporate to achieve the saturation condition.

The inlet air mass flow rate ($\dot{m}_{air}$) has only a minor effect on the saturation length (Figure 12). A lower mass flow results in a lower amount of water that needs to be evaporated for saturation. The air mass flow rate has also no effect on pressure loss, since the gas velocity is rather low (1 m/s).

The pressure (*pressure*) has a large effect on the saturation length (Figure 12), however variations of 30% on the total pressure are rather large. A different saturator inlet pressure has only a minor effect on pressure changes (Figure 13).

Finally, simulations showed that the orientation of the saturator has no effect at all on the saturation length. The orientation of the tower has also no effect on the pressure in the entrance region, but after this region, the effect

of gravity is visible on the pressure change, however rather small (300 Pa for case (a) from Figure 3, 250 Pa for case (b) and finally 200 Pa for case (c)).

*3.2.2. Counter-current*

The saturation length of the counter-current water injection is more sensitive to parameter variations (Figure 14) compared to co-current injection (Figure 12), while the pressure variations are less sensitive (Figure 15 versus Figure 13). For some variations of several parameters, no saturation was reached within the tower length or droplets did not even reached the end of the tower, resulting in no depicted results. This clearly highlights the narrow margin for counter-current droplet injection. For the sensitivity analysis of the counter-current model, the same inlet and boundary conditions as in Table 1 and 3.1.2 are used.

The droplet diameter, velocity, water mass flow and saturator length have the largest effect on the humidification process (Figure 14). If the droplets are too large, saturation is not reached inside the saturator. But on the other hand, too small droplets with a low velocity, will not reach the end of the tower, due to friction with the gas. In this case, droplets are stopped, will coalesce and fall down, depending on the orientation of the tower. The higher the velocity, the faster the droplets will move through the saturator. So the compressed air has no time to saturate. With a too low velocity, however, it is possible that the droplets will not reach the saturator exhaust. The saturator diameter has the same effect as the droplet velocity (see Figure 14), since the saturator diameter will change the gas velocity. A too large section will make the droplets pass too fast, while a too small section results in too high gas velocity and coupled friction, which augments the risk for droplet stagnation. The water mass flow rate determines the contact area between gas and water and it has a direct effect on saturation length. The saturator length is also of great importance, as shown in Figure 14. If the saturator is too short, the residence time of the droplets is not long enough to saturate the air. A too long tower however increases the risk of droplet stagnation. The effect of water and air temperature and air mass flow rate is limited. Finally, orientation has a minor effect on the saturation process.

All parameters that influence the contact area (like droplet diameter and water mass flow rate) and the velocity difference between the gas and water phase (droplet velocity, saturator diameter and tower orientation), have a large influence on pressure drop, since the pressure drop is a function of these two parameters (Figure 15). Finally, in the counter-current injection

case, the gas temperature and mass flow rate have little influence on the saturation process.

*3.2.3. Cross-current*

Saturation length in the cross-current water injection is very sensitive to saturator height variations and droplet diameter (Figure 16), while droplet diameter and saturator width variations have the largest effect on pressure losses (Figure 17). In the cross-current case, inlet conditions of Table 1 and 3.1.3 have been used.

Since a larger droplet diameter results in less contact area, compressed air will never reach saturation when too large droplets are injected. Making the saturator longer as in the co-current case is in the cross-current case no option. A small droplet diameter on the other hand provides a large contact area between both the gas and the droplets. This is positive for the heat exchange and mass transfer, but has however a negative effect on the pressure loss (Figure 17).

The droplet velocity has a large effect on saturation length (Figure 16) and on pressure change (Figure 17). The velocity will determine the residence time of the droplets in the saturator and thus the available droplets in the saturator. A larger amount of droplets is beneficial for the heat and mass transfer, but result also in more friction and thus a higher pressure drop.

Changing the saturator width ($W_{\text{saturator}}$) has almost no effect on the saturation length in the cross-current case, while the height of the saturator ($H_{\text{saturator}}$) is on the other hand of great importance (Figure 16). Changing the width will only influence the gas velocity. Since the gas velocity is rather low (approximate 1 m/s), gas velocity does not change much with increasing width. The heat and mass transfer coefficient will thus vary little, resulting in no visible effect on the saturation length. The higher the saturator on the other hand, the faster full humidification is reached. A higher saturator contains more water than a lower one, since the residence time of the droplets is larger. This provides a larger surface for heat exchange. Width and height of the saturator determine the gas velocity. The higher the velocity, the higher the pressure loss will be (Figure 17).

Water mass flow rate has a large effect on saturation length (Figure 16). The higher the water mass flow rate is, the more droplets there are, so the more contact area. A higher water mass flow rate results in more droplets and higher friction forces with the gas (Figure 17).

The length of the saturator ($L_{\text{saturator}}$) has a minor effect on the saturation

length (Figure 16) and on the pressure drop (Figure 17). The droplets are distributed homogeneously along the longitudinal axis of the saturator. Making the saturator longer results in a lower droplet density per cross section and thus a smaller contact area per cross section, which explains the longer saturation length. Relative saturation length – saturation length normalized by the total tower length – remains the same.

As in the co- and counter-current case, both air and water temperature have a minor effect on the saturation length (Figure 16). Air and water temperature also have a minor effect on pressure loss (Figure 17). Higher air and water temperatures result in more evaporation, which has an effect on the gas velocity. In addition, the air temperature will influence the density, which has also an effect on the velocity.

The air mass flow rate has, as in the co-current case, a small effect on the saturation length (Figure 16). Increasing the air mass flow rate will increase the gas velocity and thus the friction, explaining the large effect of air mass flow rate on pressure drop.

Finally changing the pressure has only a minor effect on the saturation length (Figure 16). Using injection scheme (a) from Figure 5 results in a shorter saturation length (0.09 m), since in this case; the movement of the droplets through the gas core is not influence by gravity, resulting in a longer residence time than in injection type (c) from Figure 5 (0.13 m). In addition, pressure has no effect on pressure changes as indicated in Figure 17. Orientation has a small influence on the pressure loss (less than 4 Pa).

## 4. Saturator design for Turbec T100 mGT

The final goal of this paper is to design a novel spray saturation tower that could be applied on the Turbec T100 mGT. By using a spray tower, the aim is to get a lower pressure loss than in a classical tower with packing material, while not exceeding the size of a classical saturation tower.

In their research paper, Parente et al. performed simulations of a Turbec T100 mGT converted to a mHAT operations [10] to obtain the necessary saturator volume. Final simulations indicated that a total packing volume of 0.08 $m^3$ is necessary to fully humidify the compressed air of the 100 $kW_e$ mGT with a pressure drop of 400 Pa/m of packing height. Out of the simulation results for the saturator size, using empirical correlation to estimate pressure drop over cooling tower fills [30], total expected pressure drop over

the packing can be calculated. This pressure drop is in the order of magnitude of 100 Pa, which corresponds to Parente's assumption [10].

The pressure loss can be lower than for a classic packed saturation tower, by choosing carefully the dimensions of the saturator, the nozzles (who will determine droplet velocity and diameter) and the amount of circulating water. Simulations of cross-current injection of droplets have shown that the pressure drop is very limited (33 Pa). In the co-current case, depending on the droplet velocity ($C_{\mathrm{d}}$), the pressure drop is low (5 Pa, $C_{\mathrm{d,init}} < C_{\mathrm{a,init}}$) or total pressure even slightly increases (130 Pa, $C_{\mathrm{d,init}} > C_{\mathrm{a,init}}$).

The impact of the pressure loss due to the introduction of the saturator in the mHAT cycle on the electric efficiency is limited. The effect of this additional pressure loss on the efficiency can be calculated using the Aspen® simulations previously performed by the authors of this papers [12]. Adding 100 Pa additional pressure loss to the mHAT cycle results in a relative efficiency loss of 0.2%. However, due to the accuracy of natural gas flow meters (1% for typical vortex flow meters), relative changes in efficiency smaller than 1% cannot be measured [31]. Out of this limitation and since calculations have shown that the pressure drop differences between a packed and a spray saturation tower are limited, we can conclude that as long as the pressure drop is within an order of magnitude of 100 Pa, the impact on the efficiency is far below the increase of efficiency (7%).

It was decided not to use co-current injection of the droplets, to avoid supplemental auxiliary power necessary to generate the smaller droplets. Simulations have shown that for both the co- and cross-current case, using the dimensions as mentioned in 3.1.1 and 3.1.3, fully saturated air is reached after 0.20m and 0.13m. In the co-current case, droplets of 0.1 mm need to be used, while in the cross-current case, droplets of 0.5 mm could be used. In order to get smaller droplets, the injection pressure of the water over the nozzles needs to be higher. Sauter mean diameter ($d_s$) of a nozzle at a specific pressure can only be determined experimentally. Each different nozzle has its own specification. For a standard industrial nozzles (Nozzle type: CAY2970 [32]), to reduce the droplet diameter by a factor 2, the pressure needs to be increased by a factor 2 (according to measurements of the manufacturer). This implies that in the co-current case, more power is lost to the auxiliary circulation pump for water injection, 1.5 kW compared to 150W in the cross-current case. The smaller necessary droplet diameter is penalized by a relative efficiency loss of 1.5% compared to the 0.15% loss in the cross-current case due to the higher necessary auxiliary power [12]. The loss

through the auxiliaries to provide smaller droplet diameter is of greater importance than pressure drop. Therefore, co-current injection of the droplets was decided not be used.

Counter-current was excluded as a possible injection scheme for the saturation tower due to the high sensitivity of the saturation length to inlet parameters variation. Comparing simulations of counter- (Figure 10) and cross-current (Figure 11) flow shows that in both cases saturation can be reached in a 0.5m long saturator. Sensitivity analysis results of counter-current flow however showed that saturation can only be reached in a small window of boundary conditions variation. For example in case the velocity is to low, droplets will turn around, in case the velocity is too high, no saturation is reached. In the cross-current flow simulations, the final saturation length is less sensitive to variations of these inlet conditions. Since the goal is to obtain a robust design, cross-current injection is preferred.

The final design is a cross-current saturator, with the following dimensions:

- $H_{\text{saturator}} = 0.5$ m,
- $W_{\text{saturator}} = 0.3$ m,
- $L_{\text{saturator}} = 0.5$ m.

For the ease of implementation, the horizontal gas flow (Figure 5, case (c)) will be used, since according to sensitivity analysis, there is little difference between case (a) and (c) from Figure 5. The evacuation of the remaining water is moreover easier. In case (a), the water will first move downward through the saturator wall, before it can be removed. Total pressure loss over the saturator (33 Pa) is in the same order of magnitude as the packed saturator (100 Pa). The total size is equal to $0.075\text{m}^3$, which is in the same order as the packed saturator proposed by Parente et al. ($0.08\text{m}^3$) [10].

## 5. Conclusion

For this paper, a two-phase flow model is developed for designing a novel saturation tower for mHAT applications. A spray saturation tower has been chosen to reduce pressure losses. The two major boundary conditions were pressure drop and saturator volume. The aim of this study was to develop a saturator with better performance than the classical saturator with packing.

The two-phase flow model is also used to perform a sensitivity analysis to identify the parameter which variation will have the largest influence on global performance.

Simulation of Co-, counter- and cross-current two-phase flow calculations for a spray saturator gave rise to the following conclusions:

- It is possible to fully humidify the compressed air within acceptable dimensions for the mHAT application.
- Sensitivity analysis indicated droplet diameter and water flow rate as the most crucial parameters for all different flow configurations. Halving the droplet diameter results in twice the required auxiliary pump power, while doubling the water mass flow rate, also results in twice the required auxiliary power. Per 100 W required auxiliary power, electric efficiency is reduced by 0.1%.
- Pressure drop is in the same order of magnitude as the pressure drop of a classic saturator with packing material.

Based upon these results, a suggestion for saturator design has been proposed.

## 6. Prospective

The next step in the ongoing project – the conversion of a Turbec T100 recuperated mGT, installed in the lab of the Vrije Universiteit Brussel, into a mHAT – is the construction and installation of the saturation tower to humidify the air. This implies the design and construction of a cross-current saturation tower, according to the dimensions of section 4. When designing the final saturator, some technical aspect should however be kept in mind. Nozzle selection is very important, since the nozzles will determine the droplet size and thus the heat and mass exchange rate. Next to the type of nozzles, the positioning of the nozzles is important. At all cost, interference of the different spray cones should be avoided. Interfering spray cones will lead to droplet coalescence and thus larger droplets. If the droplets are too big, full humidity will not be reached inside the saturator. Spreading the nozzles can avoid droplet coalescence, but will increase the saturator size and thus the pressure drop. The final shape of the saturator should match the spray cones to obtain optimal mixing of the air and droplets. The pressure is however a limitation for shape selection. Finally, entrained droplets

travelling in the air must be separated before entering the recuperator, especially when a low water quality is used [13]. Droplets can be separated by installing a demister, however the demister should be selected carefully in order to assure full separation of the droplets while keeping the pressure drop limited.

## 7. Acknowledgement

The research was funded by the National Fund for Scientific Research (FWO).

## Nomenclature

**Abbreviations**

AHAT Advanced Humid Air Turbine
CHAT Cascaded Humidified Advanced Turbine
EvGT Evaporative Gas Turbine
GT Gas Turbine
HAT Humid Air Turbine
mGT micro Gas Turbine
mHAT micro Humid Air Turbine
ODE Ordinary Differential Equation
REVAP® REgenerative EVAPoration
TIT Turbine Inlet Temperature
WAC Water Atomizing inlet air Cooling

**Symbols**

$\dot{m}$ mass flow rate, [kg/s]
$\dot{Q}$ heat exchange rate, [J/s]
$A$ cross section, [m$^2$]
$C$ velocity, [m/s]
$D$ diameter, [m]
$d$ droplet diameter, [m]
$d_s$ Sauter mean diameter, [m]
$F$ force, [N]
$H$ height, [m]
$h$ specific enthalpy, [J/kg]
$L$ length, [m]
$n$ amount of droplets

$p$ pressure, [Pa]
$T$ temperature, [K]
$W$ width, [m]
$x$ position along the axis of the saturator parallel to the flow direction of the compressed air, [m]

**Subscripts**

air compressed air
droplet droplet
gas partially humidified compressed air
$i$ component (film, droplets or gas core)
init initial
l loss
s source
saturator saturator
water water

**Superscripts**

$'$ per unit of length
$in$ ingoing flow condition
$out$ outgoing flow condition

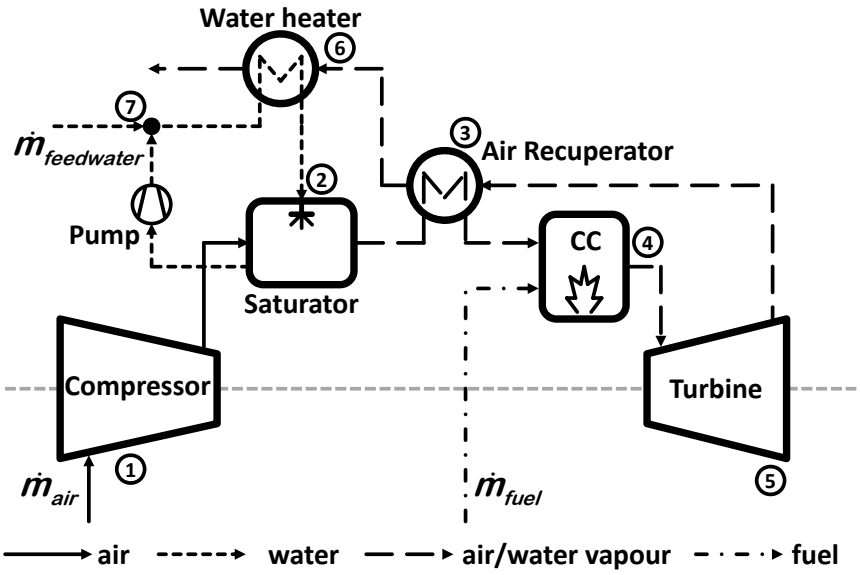


Figure 1: The mHAT, based on the original Turbec T100 mGT layout, involves next to the compressor (1), the combustion chamber (4) and the turbine (5), a saturator (2) to humidify the compressed air before preheating in the recuperator (3). The water heater (6) is used to provide the necessary hot water for the saturator. Evaporated water is replaced by feed water (7).

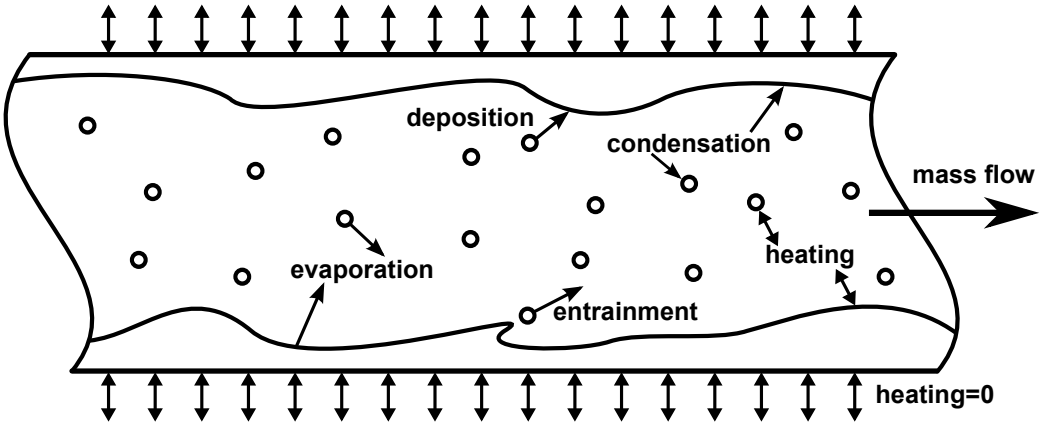


Figure 2: Annular dispersed 2-phase flow phenomena covering heat exchange and mass transfer between the different phases; through evaporation, condensation, entrainment and deposition of droplets.

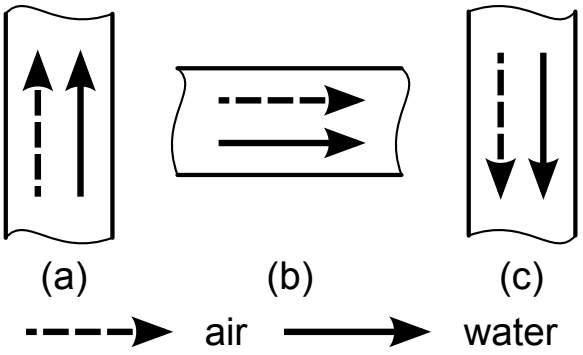


Figure 3: We evaluated these layouts of a co-current saturator: upwards (a), horizontal (b) and downwards (c) injection, to investigate the importance of gravity.

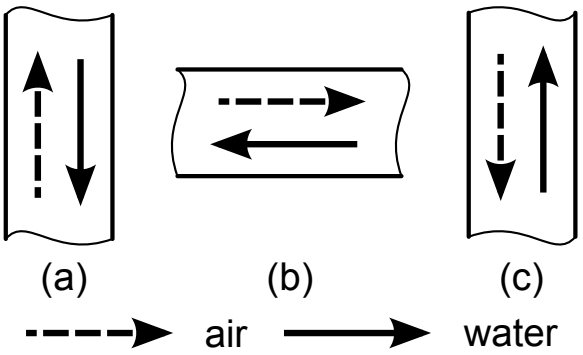


Figure 4: Evaluated layouts of a counter-current saturator, based on gas flow direction: upwards (a), horizontal gas flow (b) and downwards (c).

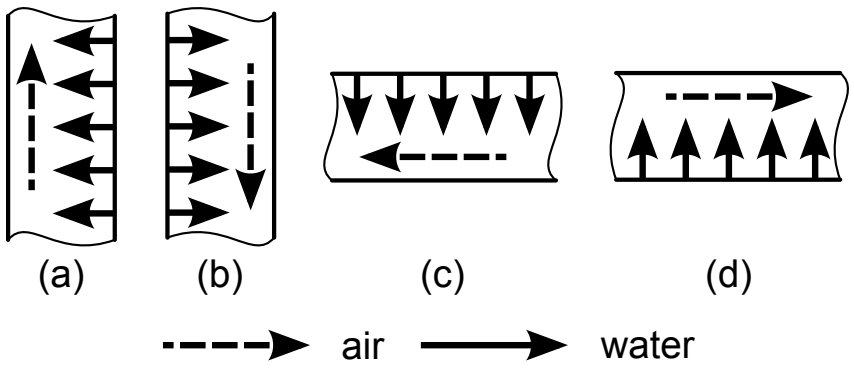


Figure 5: Possible injection schemes for a cross-current saturator, based on gas flow direction: upwards (a), downwards (b), horizontal - droplets injected downwards (c) and horizontal - droplets injected upwards (d).

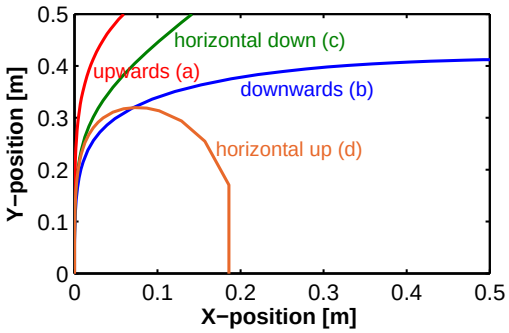


Figure 6: Droplet flow trajectory simulations indicating droplet displacements in the x-direction (compressed air flow direction) are limited (respectively 0.06 m and 0.14 m) for injection scheme (a) and (c) for a cross-current saturator, which confirms the hypothesis of droplets standing still.

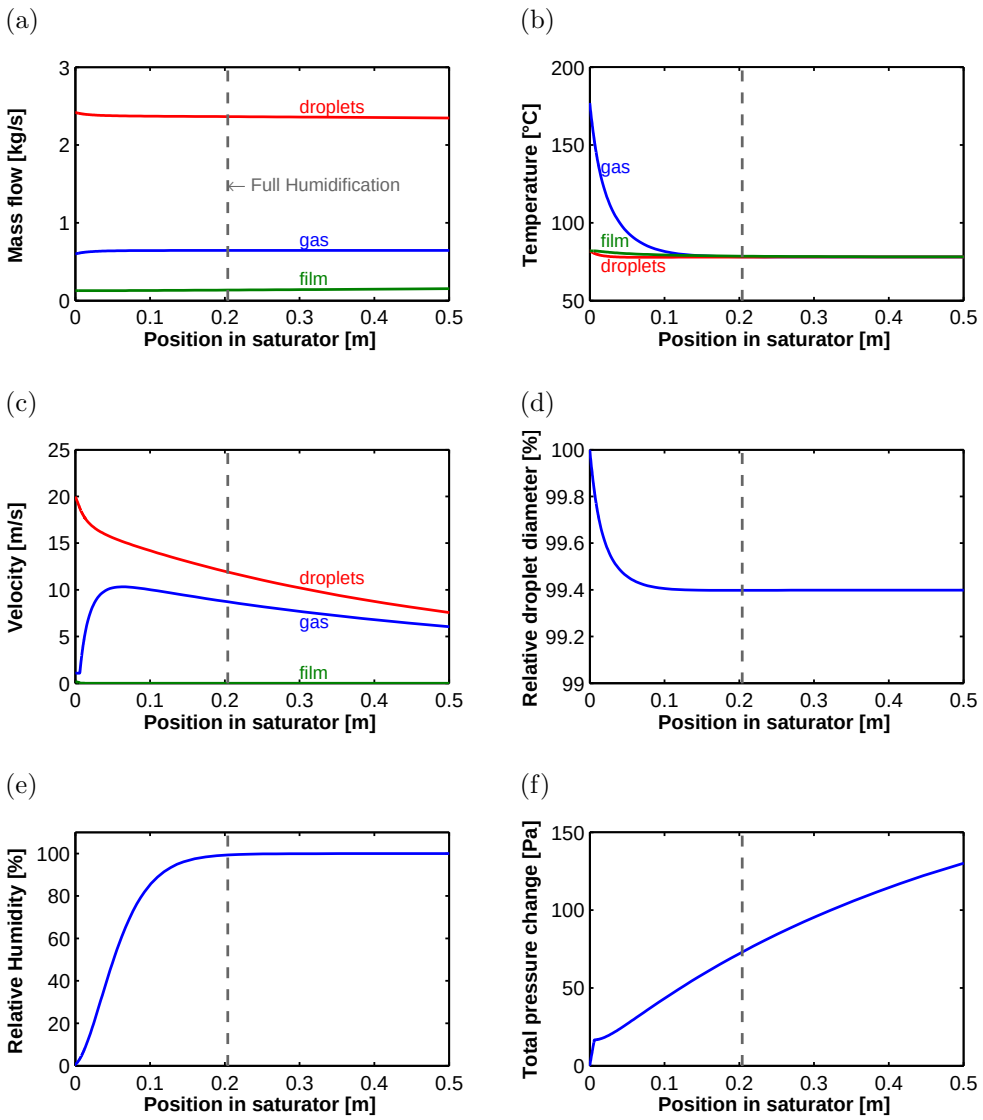


Figure 7: Simulation results of a co-current saturator, indicating necessary tower length for fully saturated air is 0.20 m.

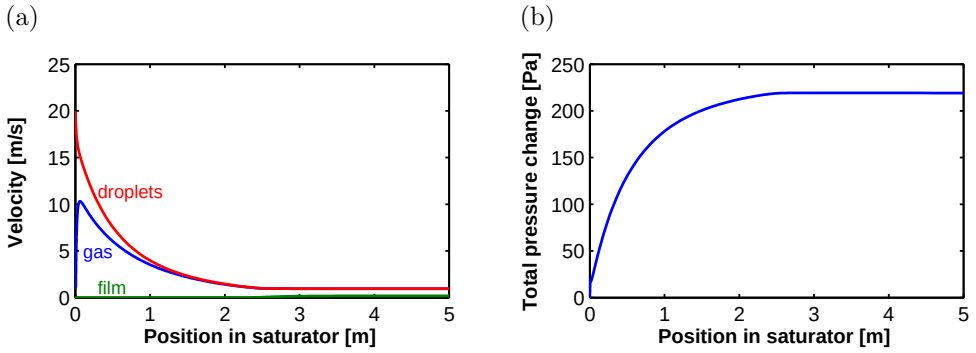


Figure 8: Velocity (a) and pressure (b) results in extended (5 m) saturator where initial droplet velocity is larger than the initial gas velocity.

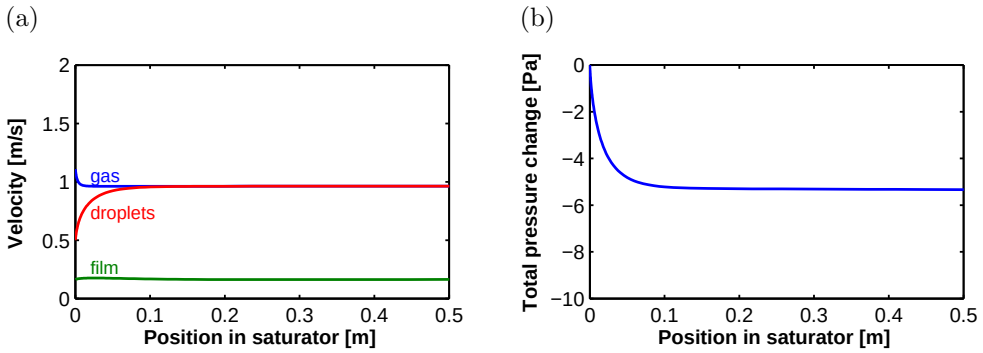


Figure 9: Velocity (a) and pressure (b) results in saturator where initial droplet velocity is lower than the initial gas velocity.

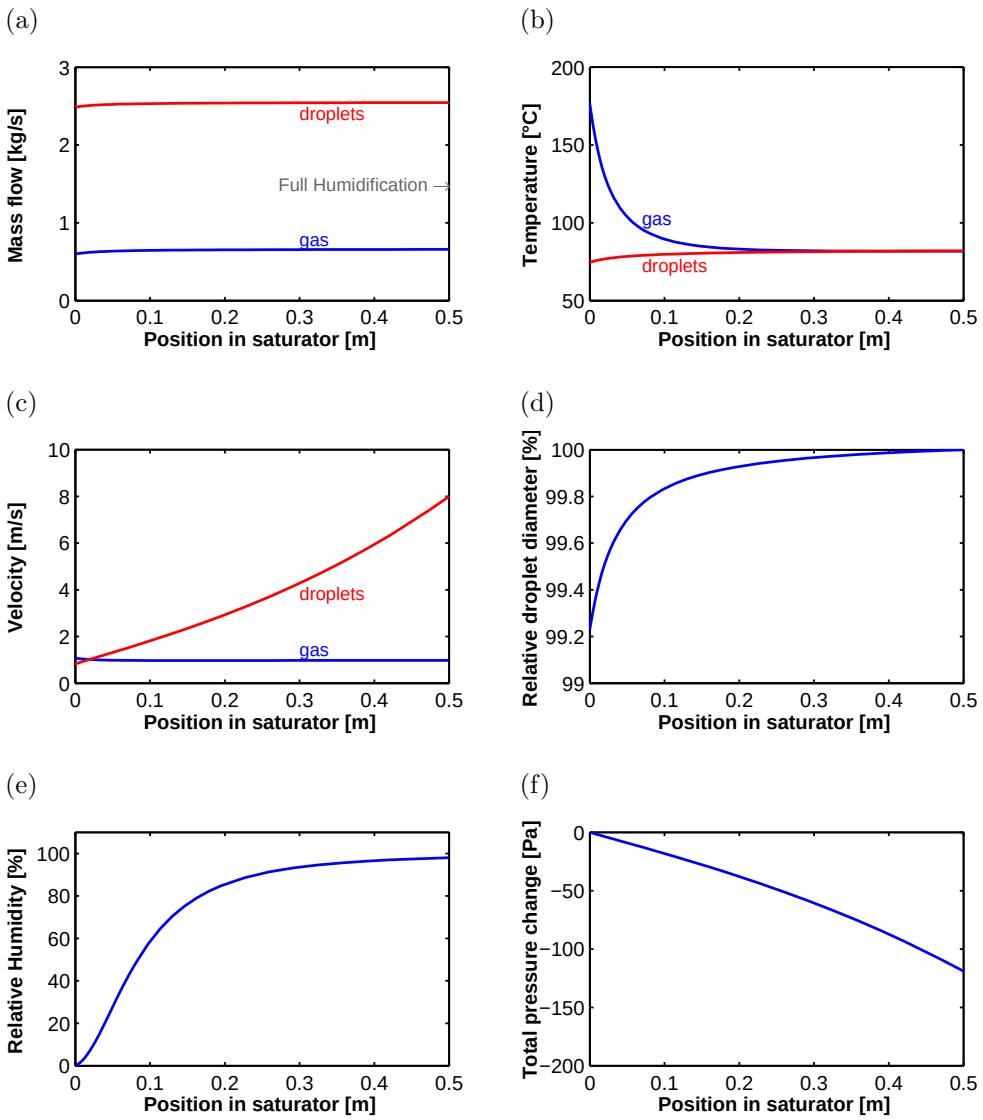


Figure 10: Simulation results of a counter-current saturator, indicating necessary tower length for fully saturated air is 0.50 m.

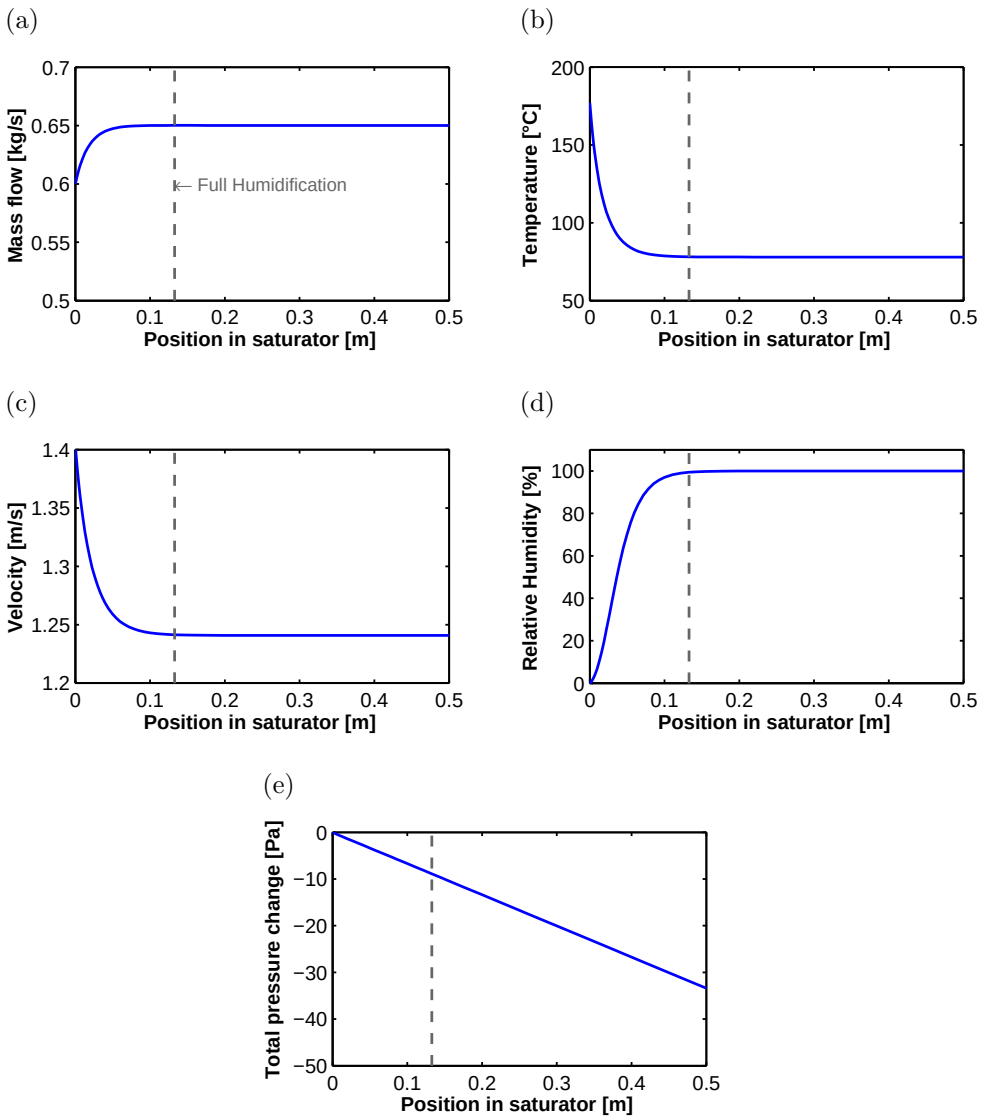


Figure 11: Simulation results of a cross-current saturator, indicating necessary tower length for fully saturated air is 0.13 m.

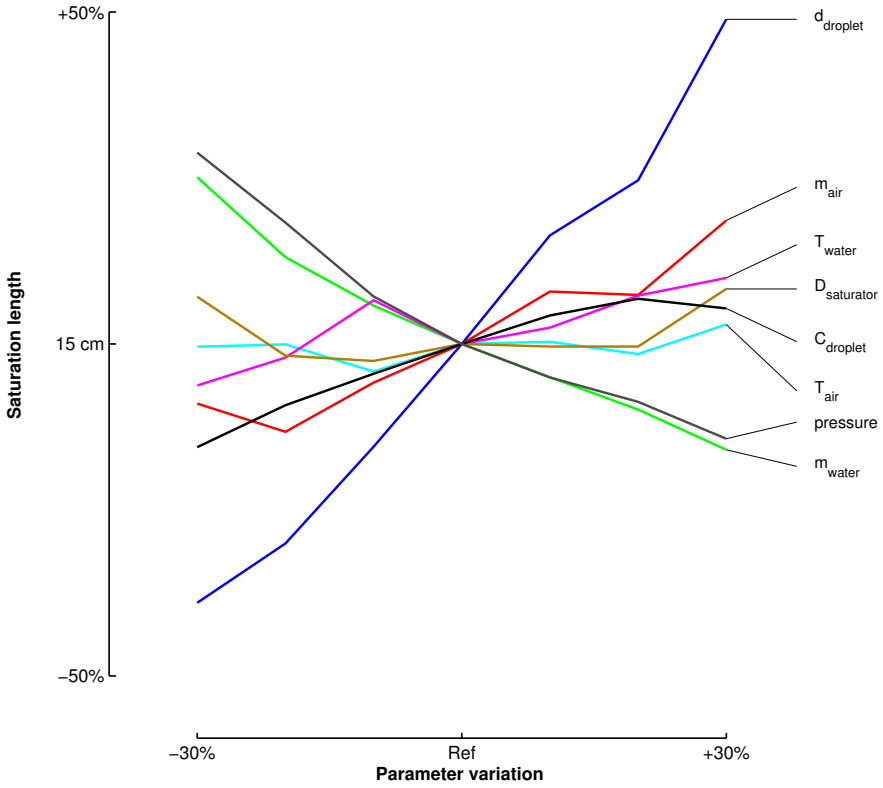


Figure 12: Results of variation of the parameters show that droplet diameter and water mass flow rate are the most crucial parameters for humidification length in co-current injection.

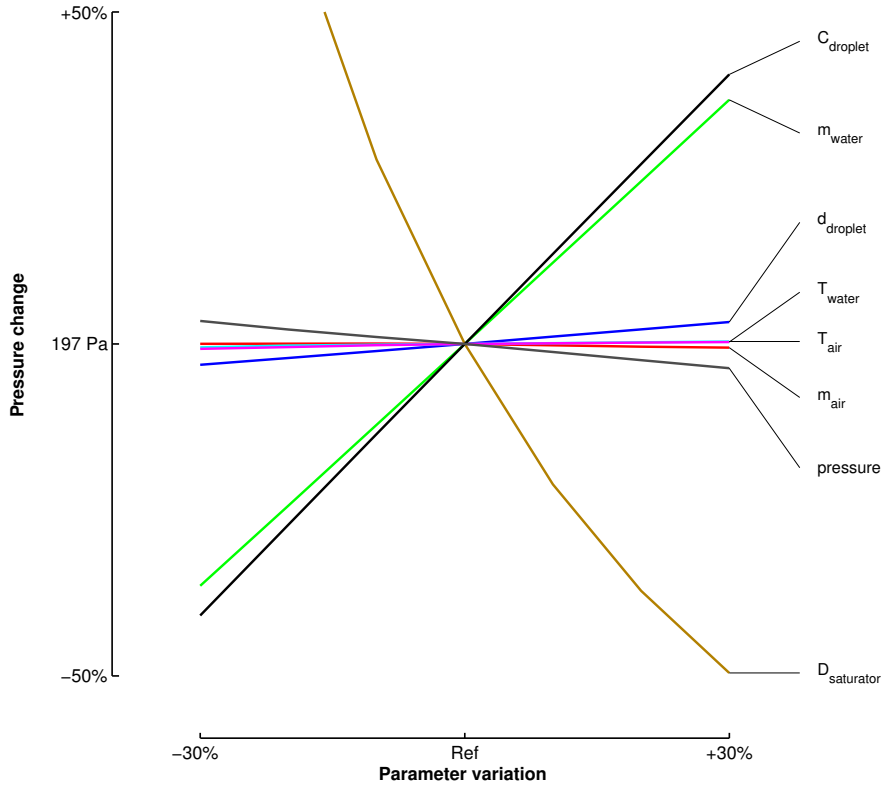


Figure 13: Results of variation of the parameters show that water mass flow rate and saturator diameter have the largest effect on total pressure change in co-current injection.

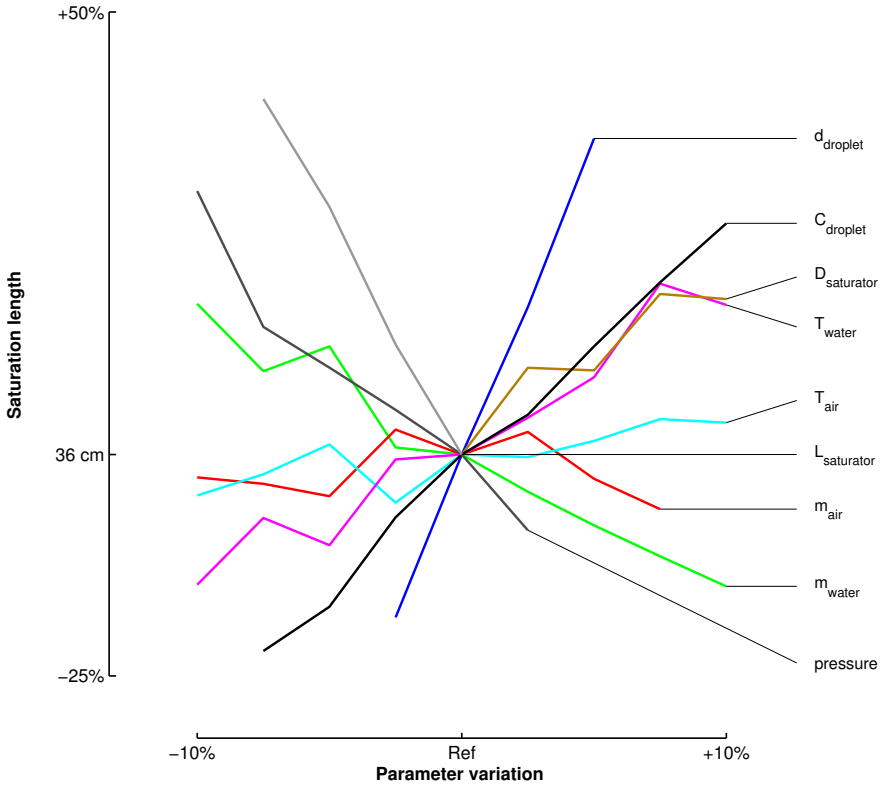


Figure 14: Results of variation of the parameters in counter-current injection, showing that droplet diameter, velocity, water mass flow and tower length are the most crucial parameters for humidification length.

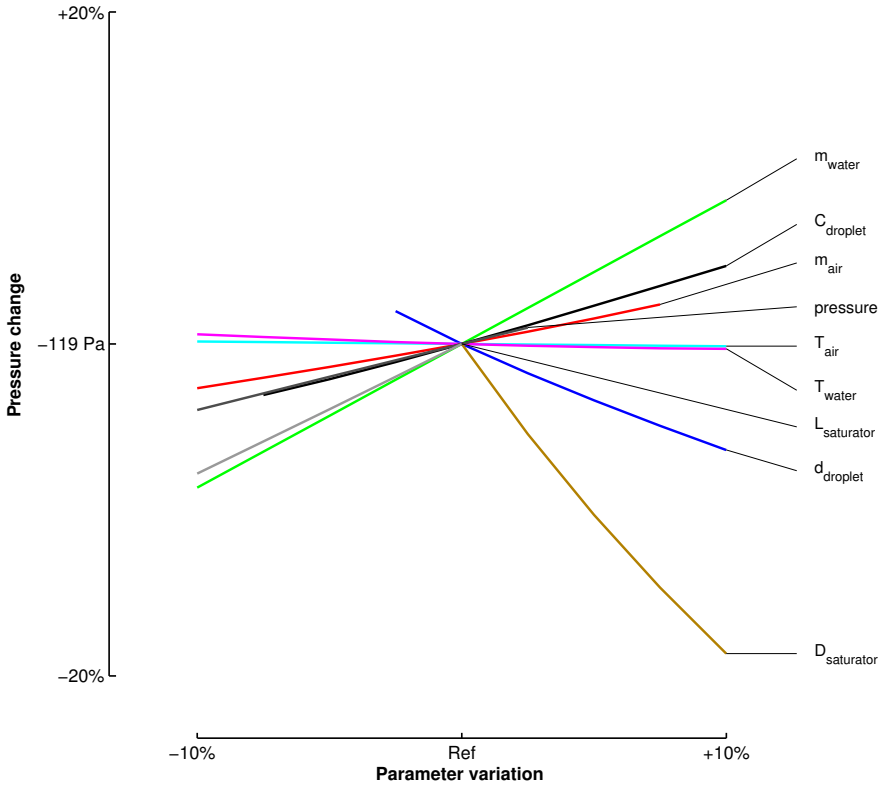


Figure 15: Results of variation of the design parameters in counter-current injection show that droplet velocity, water mass flow rate and tower width have the largest effect on total pressure change.

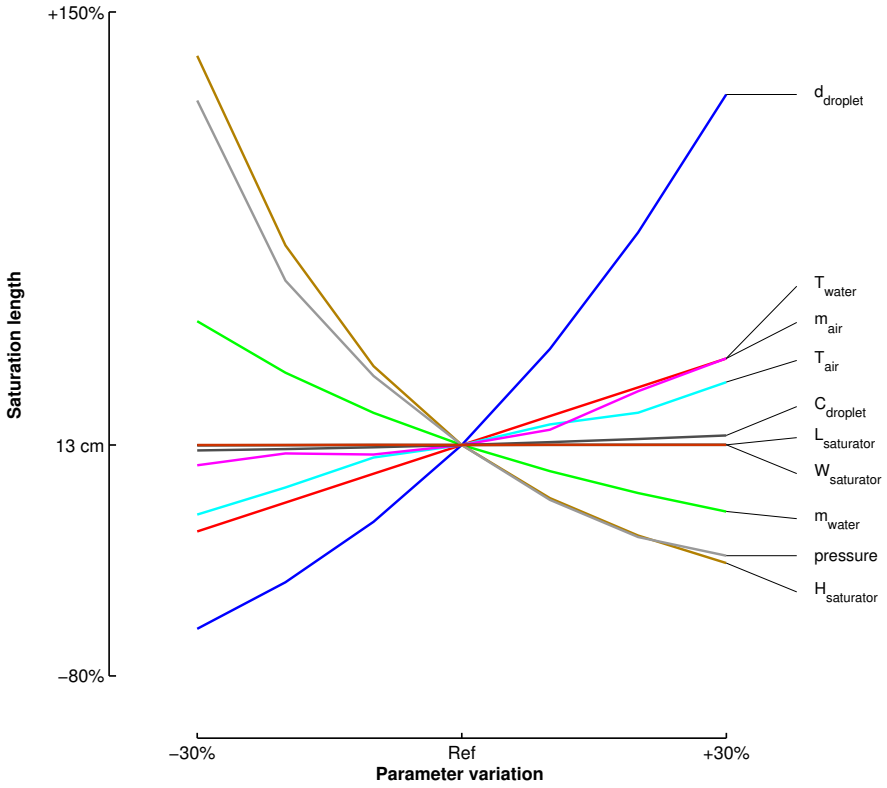


Figure 16: Results of variation of the parameters showing droplet diameter, tower height and water mass flow rate are the most crucial parameters for humidification length in cross-current injection.

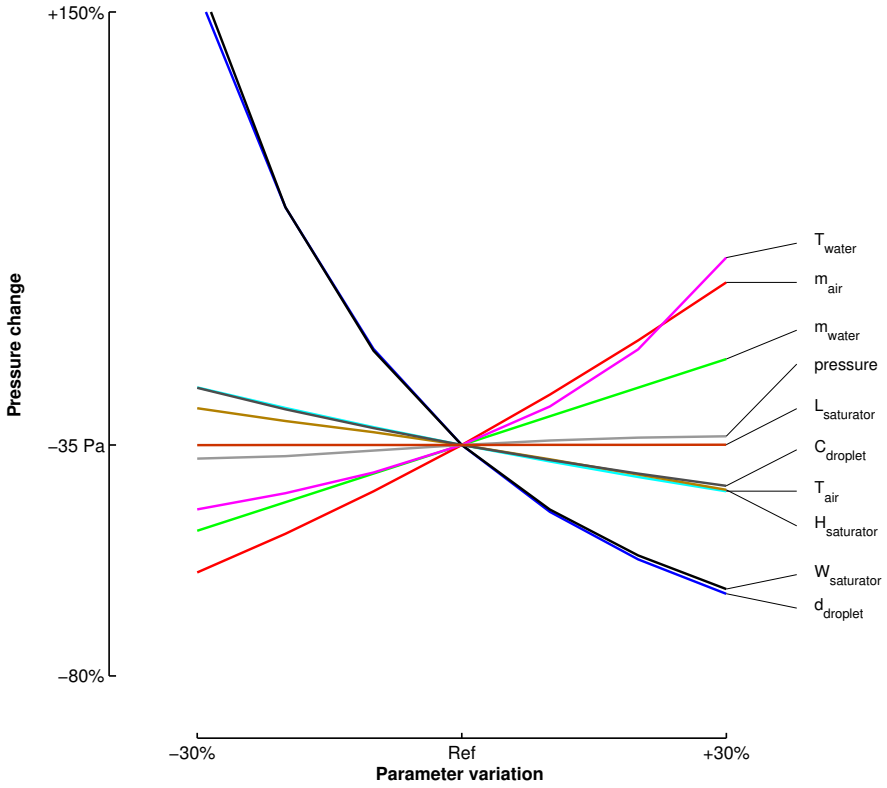


Figure 17: Results of variation of the design parameters in cross-current injection show that droplet diameter, cross section and tower length and width are the most crucial parameters for total pressure change.

Table 1: Inlet conditions of the saturator [12].

| | **Air** | | **Water** | |
|---|---|---|---|---|
| | in | out | in | out |
| $\dot{m}\,[\mathrm{kg/s}]$ | 0.600 | 0.645 | 2.545 | 2.500 |
| $T\,[^\circ\mathrm{C}]$ | 177 | 78 | 82 | 78 |
| $p\,[\mathrm{bar}]$ | 3.7 | $p_{\mathrm{air}}^{out}$ [1] | $p_{\mathrm{water}}^{in}$ [2] | $p_{\mathrm{water}}^{in} = p_{\mathrm{air}}^{out}$ [3] |

[1]The pressure of the outgoing air depends on the total loss of pressure, which will be determined when designing the saturation tower.

[2]The pressure of the incoming water depends on the used nozzle to introduce the water.

[3]The pressure of the outgoing water is equal to the pressure of the outgoing air.

**List of Figures**

**List of Tables**

## References


[1] Jonsson, M., Yan, J.. Humidified gas turbines – a review of proposed and implemented cycles. Energy 2005;30(7):1013 – 1078.

[2] Rao, A.D.. Process for producing power. US patent no. 4829763. 1989.

[3] Ågren, N.D., Westermark, M.O., Bartlett, M.A., Lindquist, T.. First experiments on an evaporative gas turbine pilot power plant: Water circuit chemistry and humidification evaluation. Journal of Engineering for Gas Turbines and Power 2002;124(1):96–102.

[4] Nakhamkin, M., Swensen, E.C., Wilson, J.M., Gaul, G., Polsky, M.. The Cascaded Humidified Advanced Turbine (CHAT). Journal of Engineering for Gas Turbines and Power 1996;118(3):565–571.

[5] Higuchi, S., Hatamiya, S., Araki, H., Marushima, S.. A study of performance on Advanced Humid Air Turbine systems. Journal of the Gas Turbine Society of Japan 2006;34(1):54–61.

[6] Dodo, S., Nakano, S., Inoue, T., Ichinose, M., Yagi, M., Tsubouchi, K., et al. Development of an advanced microturbine system using humid air turbine cycle. In: ASME conference proceedings. ASME paper GT2004-54337; 2004, p. 167–174.

[7] Higuchi, S., Koganezawa, T., Horiuchi, Y., Araki, H., Shibata, T., Marushima, S.. Test results from the Advanced Humid Air Turbine system pilot plant: Part 1–overall performance. In: ASME conference proceedings. ASME paper GT2008-51072; 2008, p. 691–700.

[8] Araki, H., Koganezawa, T., Myouren, C., Higuchi, S., Takahashi, T., Eta, T.. Experimental and analytical study on the operation characteristics of the AHAT system. Journal of Engineering for Gas Turbines and Power 2012;134:051701 (8 pages).

[9] Zhang, S., Xiao, Y.. Steady-state off-design thermodynamic performance analysis of a humid air turbine based on a micro turbine. In: ASME conference proceedings. ASME Paper GT2006-90335; 2006, p. 287–296.

[10] Parente, J., Traverso, A., Massardo, A.F.. Micro humid air cycle: Part A – thermodynamic and technical aspects. In: ASME conference proceedings. ASME paper GT2003-38326; 2003, p. 221–229.

[11] Parente, J., Traverso, A., Massardo, A.F.. Micro humid air cycle: Part B – thermoeconomic analysis. In: ASME conference proceedings. ASME paper GT2003-38328; 2003, p. 231–239.

[12] De Paepe, W., Delattin, F., Bram, S., De Ruyck, J.. Water injection in a micro gas turbine – Assessment of the performance using a black box method. Applied Energy 2013;112:1291–1302.

[13] Lindquist, T., Thern, M., Torisson, T.. Experimental and theoretical results of a humidification tower in an evaporative gas turbine cycle pilot plant. In: ASME Conference proceedings. ASME paper GT2002-30127; 2002, p. 475–484.

[14] Ågren, N.D., Westermark, M.O.J.. Design study of part-flow evaporative gas turbine cycles: Performance and equipment sizing–Part I: Aeroderivative core. Journal of Engineering for Gas Turbines and Power 2003;125(1):201–215.

[15] Parente, J.O., Traverso, A., Massardo, A.F.. Saturator analysis for an evaporative gas turbine cycle. Applied Thermal Engineering 2003;23(10):1275 – 1293.

[16] Pedemonte, A., Traverso, A., Massardo, A.. Experimental analysis of pressurised humidification tower for humid air gas turbine cycles. Part A: Experimental campaign. Applied Thermal Engineering 2008;28(14-15):1711 – 1725.

[17] Pedemonte, A., Traverso, A., Massardo, A.. Experimental analysis of pressurised humidification tower for humid air gas turbine cycles. Part B: Correlation of experimental data. Applied Thermal Engineering 2008;28(13):1623 – 1629.

[18] Traverso, A.. Humidification tower for humid air gas turbine cycles: Experimental analysis. Energy 2010;35(2):894 – 901.

[19] Araki, H., Higuchi, S., Marushima, S., Hatamiya, S.. Design study of a humidification tower for the Advanced Humid Air Turbine system.

Journal of Engineering for Gas Turbines and Power 2006;128(3):543–550.

[20] Araki, H., Higuchi, S., Koganezawa, T., Marushima, S., Hatamiya, S., Tsukamoto, M.. Test results from the Advanced Humid Air Turbine system pilot plant: Part 2–humidification, water recovery and water quality. In: ASME conference proceedings. ASME paper GT2008-51089; 2008, p. 701–712.

[21] Lagerström, G., Xie, M.. High performance and cost effective recuperator for micro-gas turbines. In: ASME Conference Proceedings. ASME paper GT2002-30402; 2002, p. 1003–1007.

[22] Zanger, J., Widenhorn, A., Aigner, M.. Experimental investigations of pressure losses on the performance of a micro gas turbine system. Journal of Engineering for Gas Turbines and Power 2011;133(8):082302 (9 pages).

[23] Bram, S.. The thermodynamic potential of evaporative regeneration in gas turbine cycles for power production. Ph.D. thesis; Vrije Universiteit Brussel; Pleinlaan 2, 1050 Brussels, Belgium; 2002.

[24] De Ruyck, J., Bram, S., Allard, G.. REVAP® cycle: A new evaporative cycle without saturation tower. Journal of Engineering for Gas Turbines and Power 1997;119(4):893–897.

[25] Fossa, M.. A simple model to evaluate direct contact heat transfer and flow characteristics in annular two-phase flow. International Journal of Heat and Fluid Flow 1995;16(4):272 – 279.

[26] Niksiar, A., Rahimi, A.. Energy and exergy analysis for cocurrent gas spray cooling systems based on the results of mathematical modeling and simulation. Energy 2009;34(1):14 – 21.

[27] Fisenko, S., Brin, A., Petruchik, A.. Evaporative cooling of water in a mechanical draft cooling tower. International Journal of Heat and Mass Transfer 2004;47(1):165 – 177.

[28] Fisenko, S., Brin, A.. Simulation of a cross-flow cooling tower performance. International Journal of Heat and Mass Transfer 2007;50(15-16):3216 – 3223.

[29] Mathworks, . Matlab R2012a. Natick, Massachusetts U.S.A.; 2012. URL: http://www.mathworks.com/; accessed: 2014-02-28.

[30] Kloppers, J.C., Kröger, D.G.. Loss coefficient correlation for wet-cooling tower fills. Applied Thermal Engineering 2003;23(17):2201 – 2211.

[31] De Paepe, W., Delattin, F., Bram, S., De Ruyck, J.. Steam injection experiments in a microturbine – a thermodynamic performance analysis. Applied Energy 2012;97:569 – 576.

[32] PNR Benelux Inc., Groot-Bijgaarden, Belgium, . World Leader for Industrial spray Nozzles and related equipment; 2012. URL: http://www.pnr.be/; accessed: 2014-02-28.